Supplemental Movie 1. Dynamics of actin patches labeled by complementary reporters. Actin reporters driven by C155-Gal4 (single timepoints shown in **Fig. S2C**). Timelapse Z-stacks were acquired by spinning disc confocal microscopy at 4 sec/frame. Movie shows MaxIPs played at 15X live speed. The predominant structures are transient patches (quantified in **Fig. 1B-D**), though we also observed much less frequent structures that exhibited significant lateral mobility or resembled 'comet tails', and other more stable, cable-like structures. Scale bar is 5 µm. Associated with **Figs 1, S1**.

Supplemental Movie 2 Loss of nwk increases the frequency of brief actin patches. MaxIPs of spinning disc confocal timelapses of control (left) and $nwk^{1/2}$ (right) muscle 6/7 NMJs acquired at 1Hz (playback 18 fps). Nwk mutants exhibit spurious synaptic F-actin assembly. Scale bar is 5µm. Associated with **Fig 6D**.

Supplemental Movie 3. AP2α and Lifeact::Ruby partially colocalize. Timelapse Z-stacks were acquired by Airyscan imaging at 4 sec/frame.of endogenously tagged AP2α::GFP and actin patches labeled by Lifeact::Ruby driven by C155-Gal4 (single timepoints shown in **Fig. 2I**). Movie shows MaxIP played at 16X live speed. Associated with **Fig 7**.

Figure 1 S1

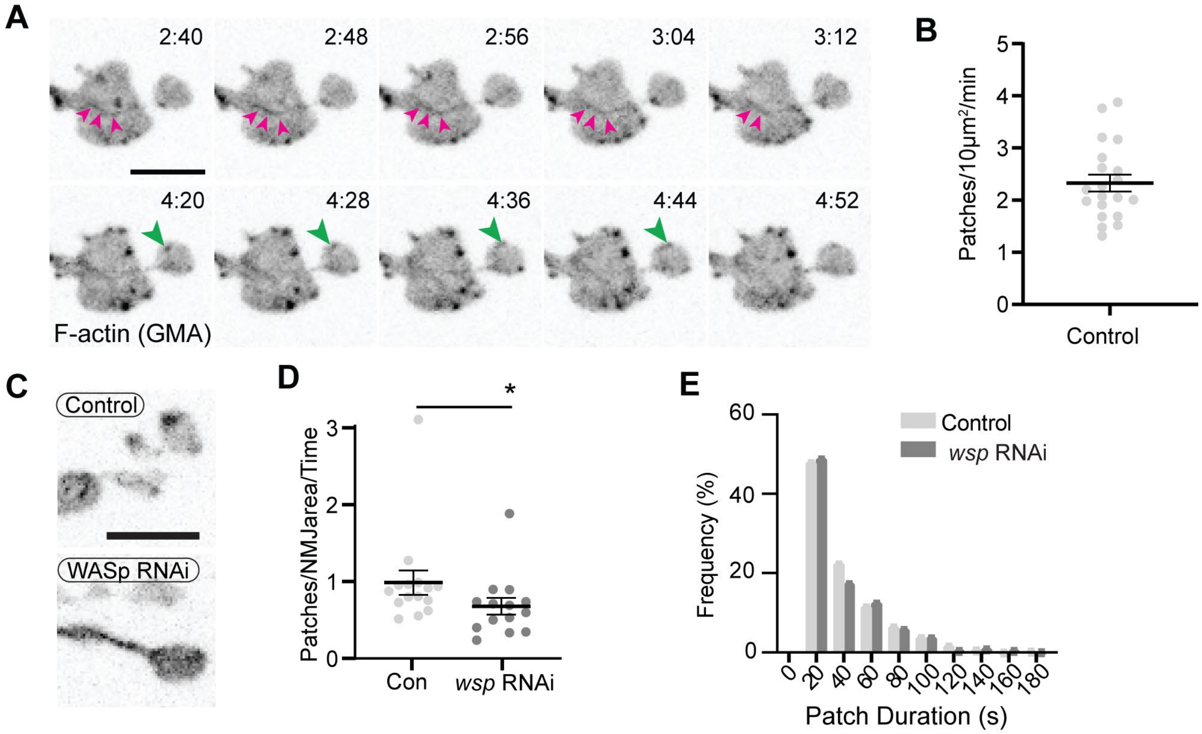

Figure 1 Supplement 1. Additional characterization of actin patches. (A) Image series from **Movie 1** highlighting actin cables (magenta arrowheads) and in addition to dynamic patches (large green arrowheads). (B) Quantification of patch frequency in NMJs expressing GMA and imaged at 1Hz. Data are from same experiment as controls in **Fig 6A-C** (C) Representative MaxIPs of single spinning disk confocal microscopy time points of neuronally expressed GMA in control and WASp RNAi (expressed in neurons via C155-GAL4) NMJs. (D,E) Quantitative analysis of patch frequency and patch duration distribution (imaged at 0.25 Hz) shows that presynaptic WASp RNAi recapitulates the decreased patch frequency observed at *WASp* mutant NMJs. Histogram bins are 20 sec; X axis values represent bin centers. Scale bars in A and C are 5 µm. Graphs show mean +/- s.e.m.; n represents NMJs. Associated with **Fig 1, Movie 1**.

Figure 3 S1

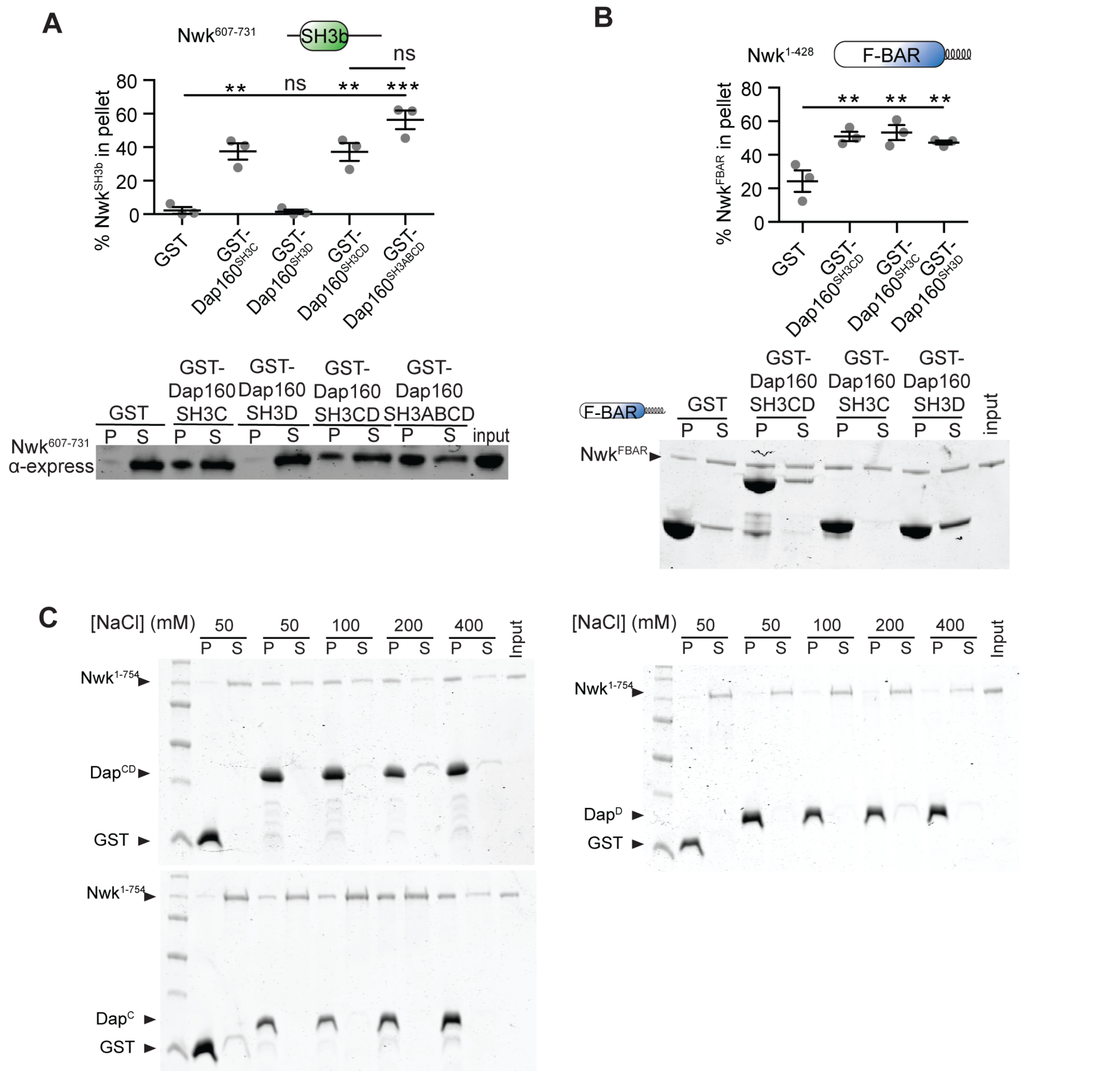

Figure 3 Supplement 1. (A-B) GST fusion proteins were immobilized on glutathione agarose and incubated with the indicated purified proteins. Pellets and supernatants were fractionated by SDS-PAGE, immunoblotted (A) or Coomassie stained (B) and quantified by densitometry. (A) Nwk^{SH3b} interacts directly with $Dap160^{SH3C}$, $Dap160^{SH3CD}$ or $Dap160^{SH3ABCD}$, but not with $Dap160^{SH3D}$ alone. $[Nwk^{SH3b}]$=7μM. (B) The Nwk F-BAR domain interacts directly with $Dap160^{SH3}$, $Dap160^{SH3D}$, and $Dap160^{SH3CD}$. $[Nwk^{F\text{-}BAR}]$=1.5μM, $[GST\text{-}Dap160^{SH3CD}]$=8.5μM, $[GST\text{-}Dap160^{SH3C/D}]$=11μM. (C) Representative Coomassie-stained gels for **Fig 3B.**

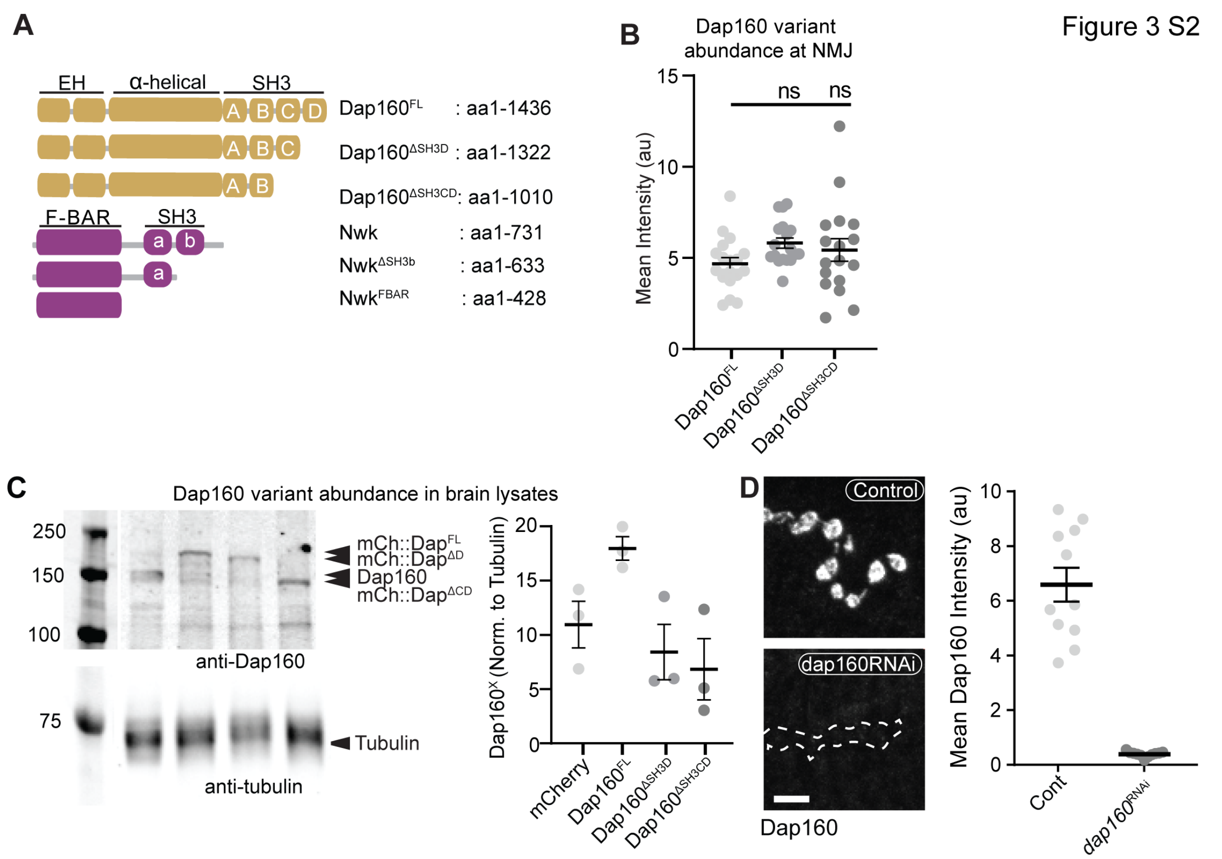

Figure 3 Supplement 2. (A) Schematic of Dap160 rescue transgenes used *in vivo* and Nwk fragments used *in vitro* experiments. (B) Quantification of Dap160 variant transgene expression (mCherry signal) at NMJs from dataset in **Fig 3E**. All transgenes were expressed in neurons by C155-GAL4 in a *dap160* null background (*dap160*$^{\Delta 1/Df}$). (C) Representative Western blots (left) and quantification (right) of Dap160 rescue transgene expression in *Drosophila* adult head extracts. (D) MaxIPs (left) and quantification (right) of spinning disc confocal micrographs of control and *dap160* RNAi expressing NMJs showing knockdown of Dap160 protein levels, using the same conditions as in **Fig 3D**. Associated with **Fig 3**.

Figure 5 S1

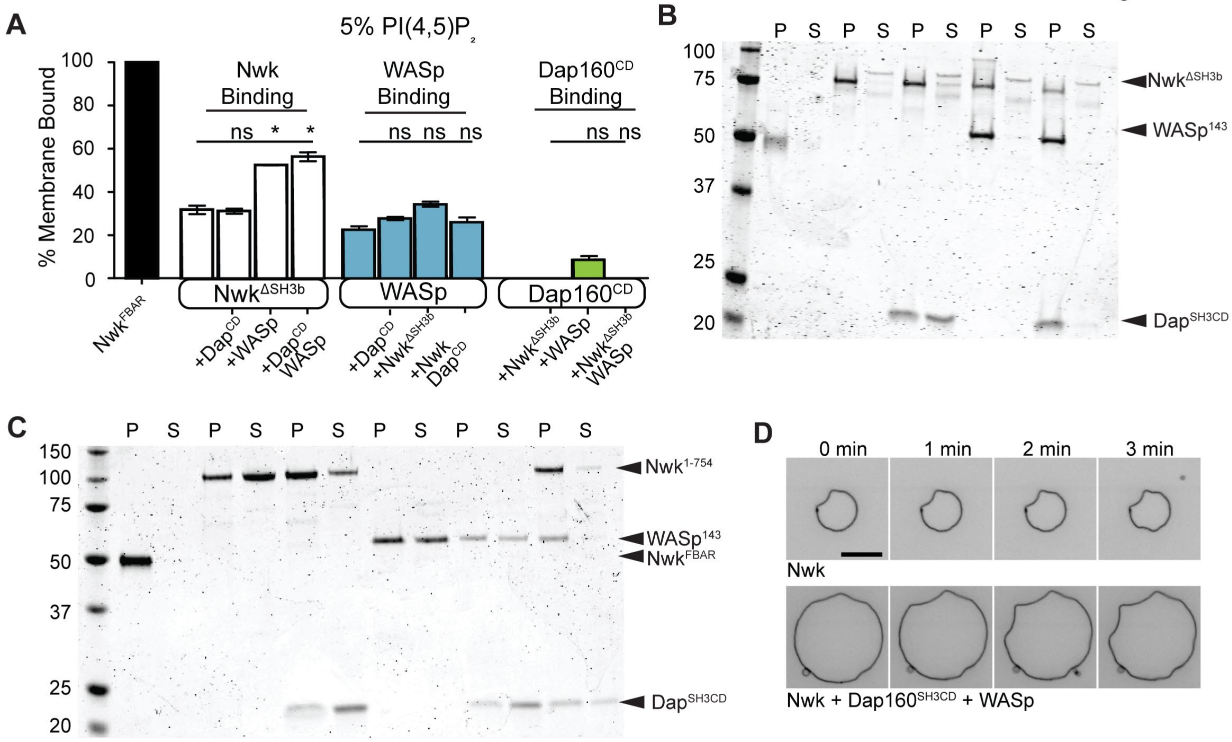

Figure 5 Supplement 1. (A) Cosedimentation assay between the indicated purified proteins and liposomes composed of [mol% = DOPC/DOPE/DOPS/PI(4,5)P_2 = 75/15/5/5]. Dap160^{SH3CD} is unable to enhance membrane binding of Nwk$^{\Delta SH3b}$ (which lacks the autoinhibitory and Dap160-binding SH3b domain), or WASp. Conversely, Nwk$^{\Delta SH3b}$ is unable to promote membrane recruitment of Dap160^{SH3CD}. Quantification from Coomassie-stained gels represents the mean fraction of total protein that cosedimented with the liposome pellet, ± SEM. [Nwk$^{1\text{-}xxx}$] = 2µM, [Dap160] = 6µM. Graph shows mean +/- s.e.m. (B) Representative Coomassie-stained gel from (A). (C) Representative Coomassie-stained gel from **Fig 5C**. (D) Confocal timelapse of deformation of GUVs (10% PI(4,5)P_2, labeled with <1% TopFluor-PE) decorated with the indicated proteins [Nwk$^{1\text{-}xxx}$] = 250 nM, [WASp]=250 nM, [Dap160] = 1.2 5µM. The Nwk-Dap160-WASp complex retains the same membrane remodeling activity as Nwk alone. Associated with **Fig 5**.

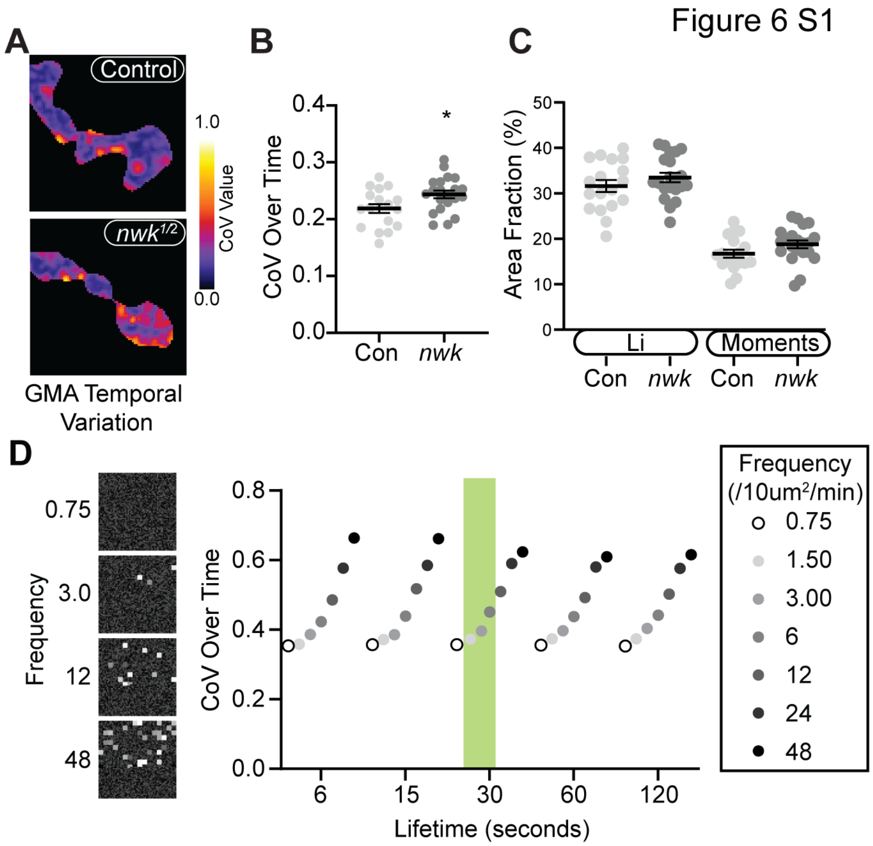

Figure 6 Supplement 1. (A) CoV projections of time-lapse movies of GMA dynamics in control and nwk mutant NMJs (analysis of same dataset as shown in 6A-C; different representative images shown). (B) Average temporal CoV values across NMJs. *nwk* mutants exhibit greater temporal variation in GMA signal than controls. (C) Quantification of the fraction of NMJ area covered by 'high' CoV pixels (identified by automated thresholding using either Li (Li and Tam, 1998) or Moments (Tsai, 1995) algorithms). *nwk* mutants show no difference in the fraction of high CoV pixels, suggesting that actin dynamics are confined to a restricted region of the synapse, and vary more over time rather than space. (D) Example of results from temporal CoV analysis of synthetic data, in which the frequency and lifetime were systematically varied. (Left) Representative images of synthetic data created using a custom FIJI script. (Right) Quantification of CoV over time. Shaded green region indicates values that most closely match in vivo measurements drawn from Patchtracker particle-based analysis. In this regime, our model indicates that the *nwk* mutant effect size in panel B corresponds to a 43% increase in patch frequency, slightly higher than the particle-based measurement of 28%.

Figure 7 S1

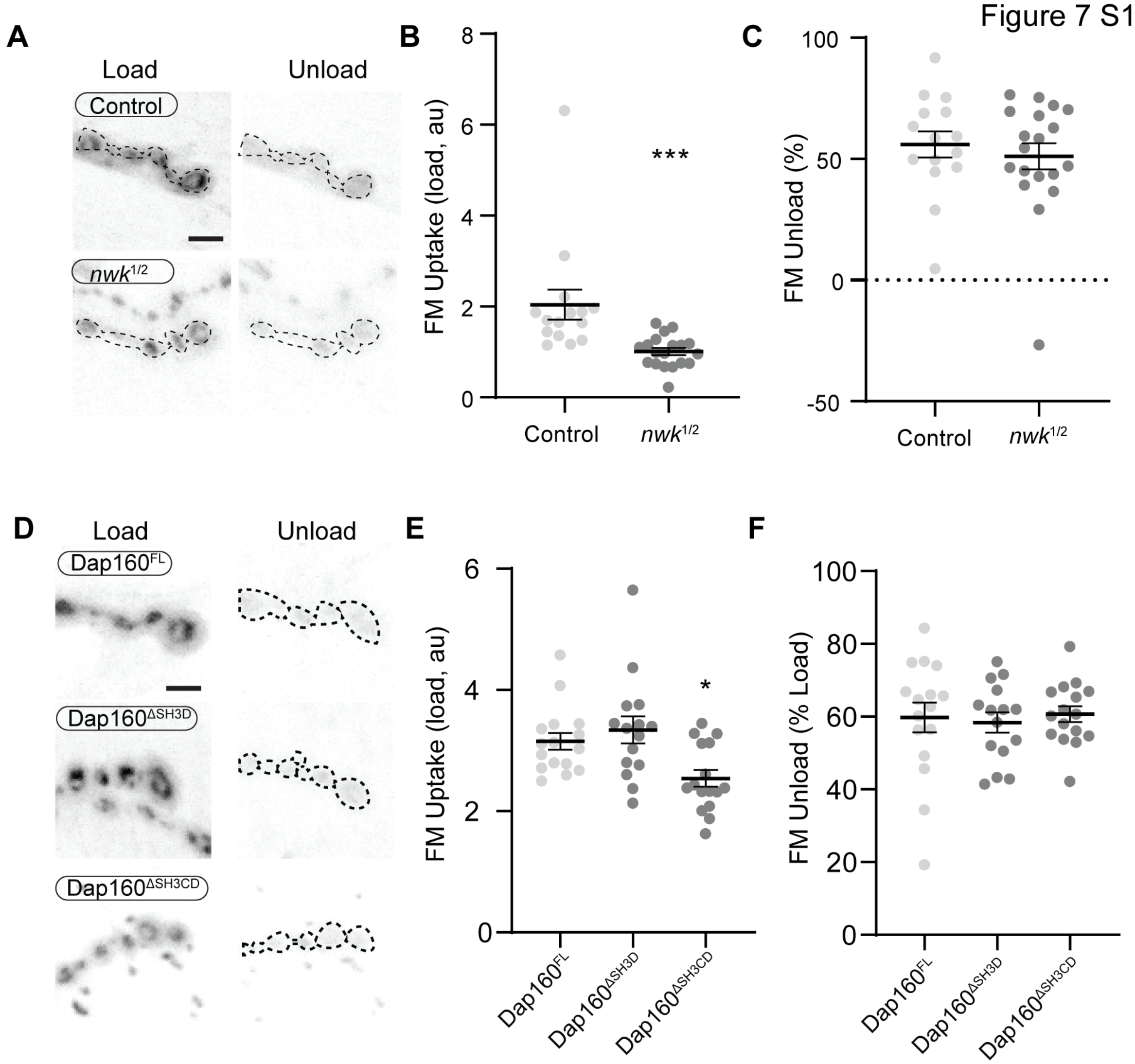

Figure 7 Supplement 1. Nwk and Dap160SH3 mutants do not disrupt FM dye unloading. Loading and unloading of FM dyes in *nwk* and *dap160*^{SH3} mutants by stimulation in 90mM KCl + 2mM $CaCl_2$. (A,D) MaxIPs of spinning disc confocal stacks acquired after loading (left) and unloading (right) of FM dyes. (B-C) Quantification of FM4-64 loading (B) and unloading (C) in *nwk* mutants. (E-F) Quantification of FM1-43 loading (E) and unloading (F) in *dap160* domain mutants.

Figure 7 S2

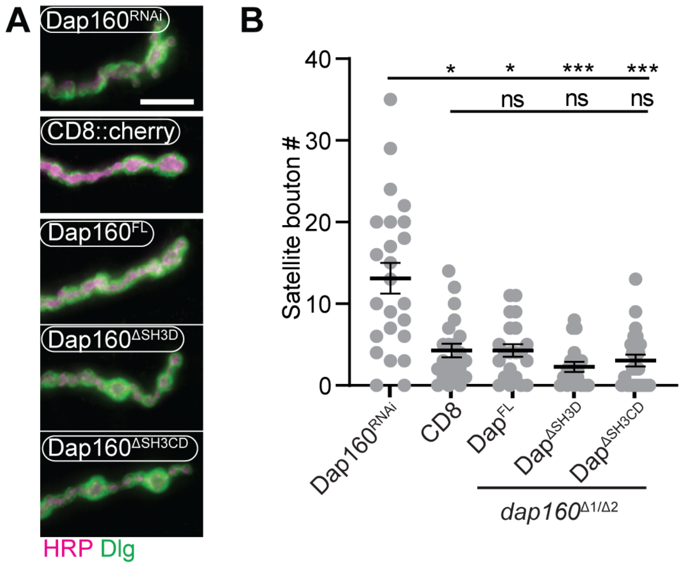

Figure 7 Supplement 2. (A-B) All Dap160 transgenes rescue *dap160* satellite bouton phenotype. (A) MaxIPs of epifluorescence micrographs of muscle 4 NMJs stained for anti-HRP (magenta) and anti-Dlg (green). $Dap160^{RNAi}$ expressing NMJs exhibit many satellite boutons, which are restored to normal levels by presynaptic expression of $Dap160^{FL}$, $Dap160^{\Delta SH3D}$, or $Dap160^{\Delta SH3CD}$ (in $dap160^{\Delta 1/Df}$ larvae). (B) Quantification of satellite boutons. Graph shows mean +/- s.em.; n represents NMJs. Scale bar in (A) is 10 µm. Associated with **Fig 7**.

Supplemental Table 1. Summary of genotypes and statistics for all experiments in this study.

Figure/ Experiment	**Genotype/Conditions**	**N**	**Statistical Test(s)**
1A-D GFP::Actin GMA Lifeact::Ruby	 C155-GAL4/+ or Y; UAS-GFP::actin/+ C155-GAL4/+ or Y; UAS-GMA/+ C155-GAL4/+ or Y; UAS-lifeact::Ruby/+	 823 patches/9 NMJ/5 larvae 819 patches/15 NMJ/6 larvae 363 patches/7 NMJ/3 larvae	NA
1E-F Arp3	 C155-GAL4/UAS-Arp3::GFP; UAS-lifeact::Ruby/+	 13 NMJ/3 larvae	NA
1G-I Control WASp	 C155-GAL4/+ or Y; UAS-GMA/+ C155-GAL4/+ or Y; wsp1,e,UAS-GMA/wsp1,e	 832 patches/18 NMJ/8 larvae 532 patches/15 NMJ/6 larvae	Kolmogorov-Smirnoff (G) Welch's t test (H)
S1A-B	C155-GAL4/+ or Y; UAS-GMA/+	1606 patches/20 NMJ/8 larvae	Kolmogorov-Smirnoff
S1C-E Control WASp	 C155-GAL4/Y; UAS-GMA/UAS-luciferaseRNAi C155-GAL4/Y; UAS-GMA/UAS-WASpRNAi	 709 patches/15 NMJ/6 larvae 286 patches/14 NMJ/5 larvae	Kolmogorov-Smirnoff (H) Mann-Whitney (I) t test (J)
2A	Nwk^{MIMICGFP}		
2B	Vglut-GAL4/Y; CD8::RFP/+; Nwk::GFP/+		
2C-D	C155-GAL4/Y; UAS-WASp::myc/+; UAS-GMA/+	14 NMJ/3 larvae	NA
2E-F	C155-GAL4/Y; UAS-WASp::myc/+; UAS-GMA/+	12 NMJ/3 larvae	NA
2G-I AP2	 C155-GAL4/+; UAS-lifeact::Ruby/AP2::GFP	 14 NMJ/3 larvae	NA
3B GST-X Nwk$^{1-731}$	 5μg 3μg	3 tech replicates per lane	NA
3B GST-CD Nwk$^{1-428}$ Nwk$^{1-731}$	 1.6μM CD, 1.2μM C/D 1.5μM 0.8μM	3 tech replicates per lane	NA
3D Dap^{FL} Dap$^{\Delta D}$ Dap$^{\Delta CD}$ Dap^{RNAi}	rescues=C155-GAL4/+; dap160$^{\Delta 1}$/Df3450; X X=UAS-Dap^{FL}::mCherry/+ X=UAS-Dap$^{\Delta D}$/+ X=UAS-Dap$^{\Delta CD}$/+ C155-GAL4, UAS-Dcr2/Y; UAS Dap160-RNAi/+	 18 NMJ/3 larvae 18 NMJ/3 larvae 17 NMJ/3 larvae 16 NMJ/3 larvae	ANOVA+Tukey's multiple comparison test
3E Dap^{FL} Dap$^{\Delta D}$ Dap$^{\Delta CD}$	rescues= C155-GAL4/+; dap160$^{\Delta 1}$/Df3450; X X=UAS-Dap^{FL}::mCherry/+ X=UAS-Dap$^{\Delta D}$/+ X=UAS-Dap$^{\Delta CD}$/+	 17 NMJ/3 larvae 18 NMJ/3 larvae 17 NMJ/3 larvae	Kruskal-Wallis + Dunn's multiple comparison test
3 S1A Nwk$^{607-731}$	 7μM		
3 S1B GST-X Nwk$^{1-428}$	 .375mg/mL (CD=8.5μM, C/D=11μM) 1.5μM	3 tech replicates per lane	ANOVA+Tukey's multiple comparison test

Figure/ Experiment	**Genotype/Conditions**	**N**	**Statistical Test(s)**
3S1C	Same experiment as Figure 3B	Same experiment as Fig 3B	ANOVA+Tukey's multiple comparison test
3S2B	Same experiment as Figure 3D	Same experiment as Fig 3D	ANOVA+Tukey's multiple comparison test
3 S2C mCh Dap^{FL} $Dap^{\Delta D}$ $Dap^{\Delta CD}$	 C155-GAL4/+; UAS-CD8::RFP/+ X=UAS-Dap^{FL}::mCherry/+ X=UAS-$Dap^{\Delta D}$/+ X=UAS-$Dap^{\Delta CD}$/+	 10 pooled brains/replicate, 3 biological replicates/group	NA
3 S2D Control Dap160RNAi	 vglut/Y; Nwk::GFP^{MiMIC}/UAS-luciferaseRNAi vglut/Y; UAS-dcr2/+; Nwk::GFP^{MiMIC}/$Dap160^{RNAi}$	 11NMJ/3larvae 11NMJ/3larvae	t test
4A Actin Arp2/3 WASp Nwk1-731 DapCD DapC	 2μM 50nM 50nM 500nM 2μM 2μM	 (1) 2 replicates (2) 2 replicates (3) 3 replicates (4) 3 replicates (5) 5 replicates (6) 2 replicates	ANOVA+ Tukey's multiple comparison test
4B Actin Arp2/3 WASp Nwk1-731 DapCD $PI(4,5)P_2$	 2μM 50nM 50nM 100nM 500nM 2μM 10% PI(4,5)P2 liposomes	 (1) 2 replicates (2) 2 replicates (3) 3 replicates (4) 3 replicates (5) 3 replicates	ANOVA+ Tukey's multiple comparison test
4C Nwk^{1-633} $Nwk^{1-731+}Dap^{CD}$	2μM OG-actin, 50nM Arp2/3, 50nM WASp 500nM Nwk^{1-633}::SNAP549 500nM Nwk^{1-731}::SNAP549+2μM $Dap160^{SH3CD}$	 41 droplets 22 droplets	NA
5A Nwk^{1-428} Nwk^{1-754} Dap^{CD}	DOPC/DOPE/DOPS/$PI(4,5)P_2$ = 70/15/5/10 3μM 1.125μM 1.69-6.75μM	3 tech replicates per group	ANOVA+ Tukey's multiple comparison test
5B Nwk^{1-XXX} $Dap160^{X}$	DOPC/DOPE/DOPS/$PI(4,5)P_2$ = 80-x/15/5/x 2μM 6μM	3 tech replicates per group, except 2 replicates for: 2.5%PIP2-Nwk^{1-428} 2.5%-Nwk^{1-731}+Dap^{SH3C}	ANOVA+ Tukey's multiple comparison test
5C Nwk^{1-731} WASp $Dap160^{CD}$	DOPC/DOPE/DOPS/$PI(4,5)P_2$ = 70/15/5/10 1μM 1μM 3μM	3 tech replicates per group	ANOVA+ Tukey's multiple comparison test
5D Nwk^{1-731} Nwk/WASp/Dap	5% $PI(4,5)P_2$ GUVs 500nM Nwk^{1-731}::SNAP549 250nM Nwk^{1-731}::SNAP549, 250nM WASp, 1.25μM $Dap160^{SH3CD}$	Representative from: 11 GUVs imaged 12 GUVs imaged	NA
5E-F Control Dap160RNAi	 vglut/Y; Nwk::GFP^{MiMIC}/UAS-luciferaseRNAi vglut/Y; UAS-dcr2/+; Nwk::GFP^{MiMIC}/$Dap160^{RNAi}$	 9 NMJs/4 larvae 10 NMJs/5 larvae	 One step association curve Mann-Whitney U test on taus

Figure/ Experiment	**Genotype/Conditions**	**N**	**Statistical Test(s)**
5 S1A-B Nwk$^{1-633}$ WASp Dap160^{CD}	DOPC/DOPE/DOPS/PI(4,5)P$_2$ = 75/15/5/5 1µM 2 µM 3µM	3 tech replicates per group	ANOVA+ Tukey's multiple comparison test
5 S1C Nwk$^{1-731}$ WASp Dap160^{CD}	DOPC/DOPE/DOPS/PI(4,5)P$_2$ = 70/15/5/10 1µM 1µM 3µM	3 tech replicates per group	ANOVA+ Tukey's multiple comparison test
5 S1D Nwk$^{1-754}$ WASp Dap160^{SH3CD}	DOPC/DOPE/DOPS/PI(4,5)P$_2$ = 70/15/5/10 250nM 1µM 250nM5% PI(4,5)P$_2$ GUVs	Representative from: 5 GUVs imaged 10 GUVs imaged	NA
6A-C Control *nwk*$^{1/2}$	 C155-GAL4/+ or Y; UAS-GMA/+ C155-GAL4/+ or Y; UAS-GMA, *nwk*^{2},*h*/ *nwk*^{1}	 1606 patches/20 NMJ/8 larvae 1928 patches/22 NMJ/8 larvae	 Mann-Whitney (B) Kolm.-Smirnoff (C)
6D-F FL ΔCD	C155-GAL4/+; dap160$^{\Delta1}$/Df3450; UAS-GMA/X X=UAS-Dap^{FL}::mCherry/+ X=UAS-Dap$^{\Delta CD}$/+	 1279 patches/14 NMJ/7 larvae 1937 patches/17 NMJ/7 larvae	 Mann-Whitney (E) Kolm.-Smirnoff (F)
6 S1A-C	Same data as 6A-C	As 6A-C	t-test (B) t-test (C)
7B-C	C155-GAL4/+; UAS-lifeact::Ruby/AP2::GFP	14 NMJ/3 larvae	NA
7D-E Control *shi*TS1	 C155-GAL4/Y; UAS-GMA/+ C155-GAL4, shiTS1/Y; UAS-GMA/+	 669 patches/16 NMJ/8 larvae 901 patches/19 NMJ/8 larvae	 Welch's t test (D)
7A-BF-G Control *nwk*$^{1/2}$ *shi*^{TS1}	 C155-GAL4/Y; UAS-GFP/+ C155-GAL4/Y; UAS-GFP/+; *nwk*^{1}/*nwk*^{2}*h* C155-GAL4, shi^{TS1}/Y; UAS-GFP/+	 23 NMJ/4 larvae 24 NMJ/4 larvae 23 NMJ/4 larvae	Kruskal-Wallis + Dunn's multiple comparison test
7C-DH-I Dap^{FL} Dap$^{\Delta D}$ Dap$^{\Delta CD}$ *shi*$^{TS!}$	rescues= C155-GAL4/+; dap160$^{\Delta1}$/Df3450; X X=UAS-Dap^{FL}::mCherry/+ X=UAS-Dap$^{\Delta D}$/+ X=UAS-Dap$^{\Delta CD}$/+ C155, shiTS1/Y x UAS-RFP	 32 NMJs/8 larvae 12 NMJs/3 larvae 12 NMJs/3 larvae 8 NMJs/2 larvae	Unpaired t-tests to dish-matched controls
7 S1A-C Control *nwk*$^{1/2}$	 C155-GAL4/Y; UAS-GFP/+ C155-GAL4/Y; UAS-GFP/+; *nwk*^{1}/*nwk*^{2}*h*	 15 NMJ/4 larvae 19 NMJ/5 larvae	 Mann-Whitney (B) t-test (C)
7 S1D-F Dap^{FL} Dap$^{\Delta D}$ Dap$^{\Delta CD}$	rescues= C155-GAL4/+; dap160$^{\Delta1}$/Df3450; X X=UAS-Dap^{FL}::mCherry/+ X=UAS-Dap$^{\Delta D}$/+ X=UAS-Dap$^{\Delta CD}$/+	 16 NMJs/4 larvae 15 NMJs/4 larvae 16 NMJs/4 larvae	 ANOVA+Tukey's multiple comparison test
Figure 7S2A-B DapRNAi mCh Dap^{FL} Dap$^{\Delta D}$ Dap$^{\Delta CD}$	 C155-GAL4, UAS-Dcr2/Y; UAS Dap160-RNAi/+ C155-GAL4/+; UAS-CD8::RFP/+ X=UAS-Dap^{FL}::mCherry/+ X=UAS-Dap$^{\Delta D}$/+ X=UAS-Dap$^{\Delta CD}$/+	 24 NMJ/6 larvae 22 NMJ/6 larvae 21 NMJ/6 larvae 16 NMJ/5 larvae 23 NMJ/6 larvae	 ANOVA+Tukey's multiple comparison test